Limitations of measurements of supercritical CO_2 sorption isotherms on coals with manometric equipment - an experimental case study

H. Yu[*], R. Jiang, L. Chen

School of Chemical and Environmental Engineering, Shandong University of Science and Technology, 266590 Qingdao, China

Accurate measurement of CO_2 adsorption on coals, which is useful for laboratory estimation of CO_2 sequestration potential in coal, has proven to be a complicated matter. A series of potential sources of error in CO_2 sorption measurements is provided here. The paper investigates the effect of experimental parameters, coal swelling and tmperature control on the measurement of supercritical CO_2 adsorption isotherms on coals. Accuracy of pressure and temperature sensors will obviously affect the determination of CO_2 adsorption, which is caused by the great value of CO_2 density change with pressure and temperature at a pressure of 8-10 MPa. The influnce of pressure- and temperature-sensors accuracy in the reference cell on CO_2 adsorption can be reduced by improving the experimental method, but their effects in the sample cell are difficult to improve. Coal swelling at high pressure leads to an obvious increase in CO_2 adsorption. A high error of supercritical CO_2 adsorption on coal will be caused by the temperature gradient in the sample cell due to the higher Joule-Thomson coefficient of CO_2 and the poor thermal conductivity of coal and CO_2. The errors of pressure and temperature, coal swelling and control of experimental temperature will lead to negative adsorption and change in the shape of the adsorption isotherm, worse reproducibility and repeatability of supercritical CO_2 adsorption.

Key words: CO_2, Sorption, Coal, Error analysis, CO_2 Sequestration.

INTRODUCTION

CO_2 is not only an important synthetic raw material in the chemical industry [1,2], but also one of the greenhouse gases [3]. Underground storage of CO_2 is one of several possible methods to reduce CO_2 emissions to the atmosphere [4]. CO_2 sequestration into deep unminable coal seams is a very attractive option for geologic CO_2 storage [5]. The supercritical CO_2 adsorption on coal is of great interest for estimating the CO_2 sequestration potential of coal beds and enhancing coal bed methane recovery using CO_2 injection into the coal seams [6-7]. The accurate measurement of supercritical CO_2 adsorption has proven to be a complicated matter [8-18]. Limitations of measurements of supercritical CO_2 adsorption on coals with manometric equipment have been studied in part 1 of this series by Jiang *et al.* [8].

In order to better understand the limitations of measurements of supercritical CO_2 sorption isotherms on coals with manometric equipment, this paper investigates the effect of the experimental parameters: accuracy, volume swelling of coal and temperature on CO_2 adsorption. The main purpose of this paper is to provide an interpretation of the high errors of excess adsorption increment and low repeatability of CO_2 adsorption isotherm measurements.

EXPERIMENTAL

Material

A coal sample was selected to investigate the effect of experimental parameters error and coal swelling on adsorption. The coal sample of particle size less than 0.2 mm was used for adsorption isotherm measurements as well as for analysis of the effect. Proximate analysis, total sulfur and density of the coal sample are given in Table 1.

Experimental apparatus and procedure

Experimental apparatus

Fig. 1 shows a simplified scheme of the experimental set-up for manometric CO_2 adsorption experiments. The set-up for manometric CO_2 adsorption experiments consists of two cells (sample cell and reference cell), two high-precision pressure sensors (max. pressure 25 MPa, precision of 0.25 %) and two micro Pt100 platinum resistances ($\pm$ 0.1ºC) to determine the temperature of the two cells. So, a pressure error of 0.05 MPa and temperature error of 0.1K were used to investigate the effect of pressure and temperature on sorption.

Table 1. Proximate analysis, total sulfur on air-dry basis (wt %) and density of coal sample used in the experiments

Moisture	Ash	Volatile matter	Fixed carbon	Total sulfur	Density (g/cm^3)
3.87	9.40	35.44	51.29	0.57	1.27
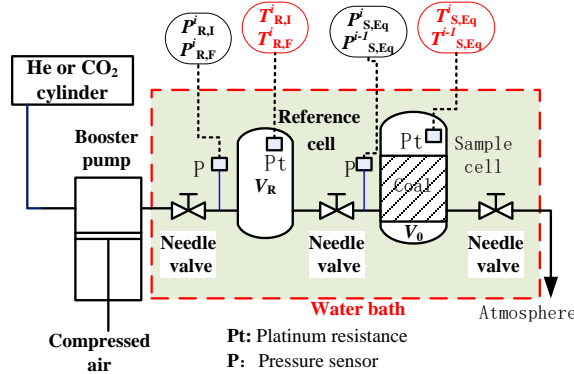
Fig. 1. Simplified scheme of the experimental setup for CO₂ sorption measurement

A booster pump driven with compressed air was used for CO_2 pressurization. The volumes of the empty reference (V_R) and sample cells were obtained by allowing helium to expand from the reference cell into the sample cell. This procedure was performed with both the empty sample cell and the sample cell filled with glass beads of a known volume for calibration. The error of V_R and V_0 is ± 0.024 cm^3 and ± 0.013 cm^3, respectively. Therefore, the estimated error in the calculation of the reference and sample cell volumes is less than 0.2%.

The standard error is 0.10 mg as quantifying sample with balance, the standard error of coal mass is 0.005 g. Table 2 shows the parameters of the experimental setup and the limits of error for each variable.

Table 2. Parameters of the experimental apparatus and limits of error, Δx, for each experimental variable

Variale	V_R (cm^3)	V_0 (cm^3)	m (g)	T (°C)	P (MPa)
x	35.4121	40.2345	10.3568	40	Table 3
Δx	0.024	0.013	0.005	0.1	0.05

Experimental procedure

CO_2 excess adsorption experiment on the coal was conducted in a programmed mode at a temperature of 40 °C and pressure up to 20 MPa.

The Gibbs-adsorption increment at the end of the ith step (Δn_i^{ex} in mmol/g) was calculated by Eq. (1).

$$\Delta n_i^{ex} = V_R \left(\rho_{R,I}^i - \rho_{R,F}^i \right)/m - V_0 \left(\rho_{S,Eq}^i - \rho_{S,Eq}^{i-1} \right)/m \qquad (1)$$

The CO_2 density (ρ) is a function of temperature (T) and pressure (P), which can be calculated with SW-EOS [19]. The pressure includes that in the reference cell before and after CO_2 expansion ($P_{R,I}^i$, $P_{R,F}^i$) in the ith step, and that in the sample cell at adsorption equilibrium ith and (i-

1)th step ($P_{S,Eq}^{i-1}$, $P_{S,Eq}^i$). The temperature values include $T_{R,I}^i$, $T_{R,F}^i$, $T_{S,Eq}^{i-1}$ and $T_{S,Eq}^i$.

$$\rho = f(P,T) \qquad (2)$$

Accuracy of supercritical CO₂ adsorption determination

The accuracy of supercritical CO_2 adsorption determination on coal is expressed with accuracy of the sensors (pressure and temperature) and other experimental parameters (volume of two cells and mass of coal sample) of manometric apparatus [8,16-17].

The expected uncertainties or errors of supercritical CO_2 adsorption inrement on coal are estimated using error propagation in all the measured variables.

$$\Delta n_i^{ex} = f(\rho, m, V) \qquad (3)$$

$$d\Delta n_i^{ex} = \sqrt{\left(\frac{\partial \Delta n_i^{ex}}{\partial \rho} \Delta \rho \right)^2 + \left(\frac{\partial \Delta n_i^{ex}}{\partial m} \Delta m \right)^2 + \left(\frac{\partial \Delta n_i^{ex}}{\partial V} \Delta V \right)^2} \qquad (4)$$

Errors of experimental parameters

The estimated error of the excess adsorption increment for the ith step caused by the error of $P_{R,I}^i$, $P_{R,F}^i$, $P_{S,Eq}^{i-1}$ and $P_{S,Eq}^i$, was calculated with Eqns. (5)-(8) based on Eqns. (1) and (2).

$$\frac{\partial \Delta n_i^{ex}}{\partial P_{R,I}^i} = \frac{V_R}{m} \left(\frac{\partial \rho_{R,I}^i}{\partial P_{R,I}^i} \right)_T \qquad (5)$$

$$\frac{\partial \Delta n_i^{ex}}{\partial P_{R,F}^i} = -\frac{V_R}{m} \left(\frac{\partial \rho_{R,F}^i}{\partial P_{R,F}^i} \right)_T \qquad (6)$$

$$\frac{\partial \Delta n_i^{ex}}{\partial P_{S,Eq}^{i-1}} = \frac{V_0}{m} \left(\frac{\partial \rho_{S,Eq}^{i-1}}{\partial P_{S,Eq}^{i-1}} \right)_T \qquad (7)$$

$$\frac{\partial \Delta n_i^{ex}}{\partial P_{S,Eq}^i} = -\frac{V_0}{m} \left(\frac{\partial \rho_{S,Eq}^i}{\partial P_{S,Eq}^i} \right)_T \qquad (8)$$

The error of the excess adsorption increment caused by the error of volume in the reference cell (V_R) and void-volume in the sample cell (V_0), was calculated with Eqns. (9) and (10) based on Eq. (1).

$$\frac{\partial \Delta n_i^{ex}}{\partial V_R} = \frac{1}{m} \left(\rho_{R,I}^i - \rho_{R,F}^i \right) \qquad (9)$$

$$\frac{\partial \Delta n_i^{ex}}{\partial V_0} = -\frac{1}{m} \left(\rho_{S,Eq}^i - \rho_{S,Eq}^{i-1} \right) \qquad (10)$$

The increment error caused by the mass of experimental coal sample is,

$$\frac{\partial \Delta n_i^{ex}}{\partial m} = -\frac{\Delta n_i^{ex}}{m} \qquad (11)$$

The increment errors caused by the error of the experimental temperatures ($T_{R,I}^i$, $T_{R,F}^i$, $T_{S,Eq}^{i-1}$ and $T_{S,Eq}^i$) are Eqns. (12)-(15) based on Eqns. (1) and (2).

$$\frac{\partial \Delta n_i^{ex}}{\partial T_{R,I}^i} = \frac{V_R}{m}\left(\frac{\partial \rho_{R,I}^i}{\partial T_{R,I}^i}\right)_P \tag{12}$$

$$\frac{\partial \Delta n_i^{ex}}{\partial T_{R,F}^i} = -\frac{V_R}{m}\left(\frac{\partial \rho_{R,F}^i}{\partial T_{R,F}^i}\right)_P \tag{13}$$

$$\frac{\partial \Delta n_i^{ex}}{\partial T_{S,Eq}^{i-1}} = \frac{V_0}{m}\left(\frac{\partial \rho_{S,Eq}^{i-1}}{\partial T_{S,Eq}^{i-1}}\right)_P \tag{14}$$

$$\frac{\partial \Delta n_i^{ex}}{\partial T_{S,Eq}^i} = -\frac{V_0}{m}\left(\frac{\partial \rho_{S,Eq}^i}{\partial T_{S,Eq}^i}\right)_P \tag{15}$$

CO_2 density change with pressure at a constant temperature, its change with temperature at a contant pressure, and density can be obtained with the SW-EoS. These relationships can now be used to determine the contribution of each parameter to the increment error.

The errors of sorption increment caused by experimental parameters can be obtained with Eqns. (3)-(13). The error limits of each parameter are obtained with the accuracy of measurement parameters shown in Table 2.

The contribution of each parameter to the expected error of the excess adsorption increment (Δn_{x_j}), were calculated using the viable value, the density changes (Table 3), Eqns. (5)-(15), and the limits of error of each variable, Δx_j (Table 2).

Standard error of excess adsorption

The estimated standard errors of excess adsorption increment caused by pressure, temperature and volume are calculated with Eqns. (16)-(18).

$$\Delta n_P = \sqrt{\left(\Delta n_{P_{R,I}^i}\right)^2 + \left(\Delta n_{P_{R,F}^i}\right)^2 + \left(\Delta n_{P_{S,Eq}^i}\right)^2 + \left(\Delta n_{P_{S,Eq}^{i-1}}\right)^2} \tag{16}$$

$$\Delta n_T = \sqrt{\left(\Delta n_{T_{R,I}^i}\right)^2 + \left(\Delta n_{T_{R,F}^i}\right)^2 + \left(\Delta n_{T_{S,Eq}^i}\right)^2 + \left(\Delta n_{T_{S,Eq}^{i-1}}\right)^2} \tag{17}$$

$$\Delta n_V = \sqrt{\left(\Delta n_{V_R}\right)^2 + \left(\Delta n_{V_0}\right)^2} . \tag{18}$$

The estimated standard error of the adsorption increment ($d\left(\Delta n_i^{ex}\right)$) can be obtained by Eq. (19) and above derivative (Eqns. (5)-(15)). The standard error of total adsorption ($d\left(n_i^{ex}\right)$) was calculated by Eq. (20).

$$d\left(\Delta n_i^{ex}\right) = \sqrt{\begin{array}{l}\left(\Delta n_{P_{R,I}^i}\right)^2 + \left(\Delta n_{P_{R,F}^i}\right)^2 + \left(\Delta n_{P_{S,Eq}^i}\right)^2 + \left(\Delta n_{P_{S,Eq}^{i-1}}\right)^2 + \left(\Delta n_{T_{R,I}^i}\right)^2 + \\ \left(\Delta n_{T_{R,F}^i}\right)^2 + \left(\Delta n_{T_{S,Eq}^i}\right)^2 + \left(\Delta n_{T_{S,Eq}^{i-1}}\right)^2 + \left(\Delta n_{V_R}\right)^2 + \left(\Delta n_{V_0}\right)^2 + \left(\Delta n_m\right)^2\end{array}} \tag{19}$$

$$dn_j^{ex} = \sqrt{\left(d\Delta n_1^{ex}\right)^2 + \left(d\Delta n_2^{ex}\right)^2 + \cdots + \left(d\Delta n_j^{ex}\right)^2} \tag{20}$$

RESULTS AND DISCUSSION

CO_2 density change

CO_2 density change at a constant temperature (T) is a partial derivative of the density (ρ) with respect to the pressure (P) variable, i.e. $[\partial \rho / \partial P]_T$, which was investigated in a former paper [17] in detail.

$$\left[\frac{\partial \rho}{\partial P}\right]_T = \frac{1}{RT\left(1 + 2\delta\phi_\delta^r + \delta^2\phi_{\delta\delta}^r\right)} \tag{21}$$

CO_2 density change at a constant pressure (P) is a partial derivative of the density (ρ) with respect to the temperature (T) variable, i.e. $[\partial \rho / \partial T]_P$.

$$\frac{P}{RT\rho} = 1 + \frac{\rho}{\rho_c}\phi_\delta^r . \tag{22}$$

Rearranging Eq. (22) gives

$$RT\rho + \frac{RT\rho^2}{\rho_c}\phi_\delta^r = P . \tag{23}$$

From Eq. (23), the partial derivative of ρ with respect to temperature (T) at a constant pressure (P) is expressed as:

$$\begin{array}{l}R\rho + RT\left(\partial\rho / \partial T\right)_P + \\ \frac{R}{\rho_0}\left[\begin{array}{l}\rho^2\phi_\delta^r + 2\rho T\phi_\delta^r\left(\partial\rho / \partial T\right)_P + \\ T\rho^2\left[\left(\partial\phi_\delta^r / \partial\rho\right)_P\left(\partial\rho / \partial T\right)_P\left(\partial\phi_\delta^r / \partial T\right)_P\right]\end{array}\right] = 0\end{array} \tag{24}$$

So, the CO_2 density change with temperature at a constant pressure is given by

$$\left[\frac{\partial \rho}{\partial T}\right]_P = -\frac{\rho}{T}\left(\frac{1 + \delta\phi_\delta^r - \tau\delta\phi_{\delta\tau}^r}{1 + 2\delta\phi_\delta^r + \delta^2\phi_{\delta\delta}^r}\right) \tag{25}$$

The description and meanings of the symbols in Eqns. (21) to (25) are detailed in document [19].

The CO_2 density change value ($[\partial\rho/\partial P]_T$ and
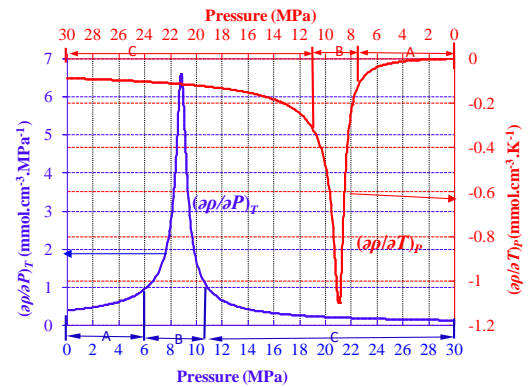
Fig. 2. CO_2 density change ($[\partial\rho/\partial P]_T$) and ($[\partial\rho/\partial T]_P$) at 40 ºC, obtained from the SW-EOS.

$\partial\rho/\partial T]_P$) at a temperature of 40℃ and a pressure up to 30 MPa is shown in Fig. 2.

Table 3 shows the experimental results and CO_2 density change.

Table 3. Experimental pressure, density and its change value calculated with SW-EOS, CO_2 adsorption and its increment obtained for the adsorption isotherm of CO_2 at $40\,°C$

i	Pressure (MPa)				Density (mmol/cm³)				Density change $(\partial\rho/\partial P)_T$ (mmol·cm⁻³·MPa⁻¹)				$(\partial\rho/\partial T)_P$ (mmol·cm⁻³·K⁻¹)				Adsorption (mmol/g)	
	$P_{R,I}^{i}$	$P_{R,F}^{i}$	$P_{S,Eq}^{i-1}$	$P_{S,Eq}^{i}$	$\rho_{R,I}^{i}$	$\rho_{R,F}^{i}$	$\rho_{S,Eq}^{i-1}$	$\rho_{S,Eq}^{i}$	$P_{R,I}^{i}$	$P_{R,F}^{i}$	$P_{S,Eq}^{i-1}$	$P_{S,Eq}^{i}$	$T_{R,I}^{i}$	$T_{R,F}^{i}$	$T_{S,Eq}^{i-1}$	$T_{S,Eq}^{i}$	Δn_i^{ex}	n_i^{ex}
(1)	(2)	(3)	(4)	(5)	(6)	(7)	(8)	(9)	(10)	(11)	(12)	(13)	(14)	(15)	(16)	(17)	(18)	(19)
1	6.236	3.873	0.001	2.500	3.670	1.857	0.001	1.108	1.018	0.601	0.384	0.497	-0.046	-0.012	0.000	-0.005	0.170	0.170
2	3.873	3.221	2.5	3.083	1.857	1.483	1.108	1.409	0.601	0.546	0.497	0.535	-0.012	-0.008	-0.005	-0.008	0.003	0.173
3	6.366	4.967	3.083	4.65	3.805	2.581	1.409	2.356	**1.063**	0.734	0.535	0.689	-0.051	-0.021	-0.008	-0.018	0.027	0.200
4	6.356	5.652	4.65	5.314	3.795	3.125	2.356	2.846	1.059	0.860	0.689	0.792	-0.050	-0.032	-0.018	-0.026	0.027	0.228
5	12.271	10.213	5.314	6.396	16.510	14.691	2.846	3.838	0.598	1.406	0.792	1.074	**-0.231**	-0.415	-0.026	-0.052	0.223	0.450
6	16.119	9.703	6.396	6.964	18.114	13.809	3.838	4.518	0.306	**2.155**	1.074	1.346	-0.150	**-0.560**	-0.052	-0.080	**1.259**	1.709
7	17.018	11.062	6.964	7.681	18.375	15.634	4.518	5.698	0.276	0.894	1.346	2.050	-0.141	-0.303	-0.080	-0.166	0.474	2.183
8	17.468	10.962	7.681	8.419	18.497	15.542	5.698	7.900	0.264	0.933	2.050	4.473	-0.137	-0.312	-0.166	-0.546	0.102	**2.285**
9	20.526	12.481	8.419	8.998	19.202	16.632	7.900	11.312	0.203	0.567	4.473	**5.672**	-0.117	-0.223	-0.546	**-1.071**	-0.568	1.717
10	19.317	13.531	8.998	9.813	18.945	17.161	11.312	14.034	0.223	0.451	**5.672**	1.935	-0.124	-0.192	**-1.071**	-0.519	-0.550	1.167
11	22.344	18.307	9.813	11.222	19.549	18.709	14.034	15.772	0.180	0.243	1.935	0.837	-0.109	-0.131	-0.519	-0.290	-0.459	0.708
12	18.307	16.289	11.222	12.701	18.709	18.166	15.772	16.753	0.243	0.300	0.837	0.537	-0.131	-0.149	-0.290	-0.216	-0.234	0.474
13	22.624	18.777	12.701	15.819	19.599	18.821	16.753	18.021	0.177	0.233	0.537	0.317	-0.108	-0.128	-0.216	-0.154	-0.275	0.198
14	23.903	21.755	15.819	17.548	19.817	19.441	18.021	18.518	0.164	0.187	0.317	0.262	-0.103	-0.112	-0.154	-0.137	-0.082	0.116
15	22.914	21.325	17.548	18.987	19.650	19.360	18.518	18.870	0.174	0.192	0.262	0.229	-0.107	-0.114	-0.137	-0.126	-0.050	0.066

There are $P_{R,I}^{i} > P_{R,F}^{i} > P_{S,Eq}^{i} > P_{S,Eq}^{i-1}$ and they are in the region A (Fig. 2) for pressure points 1 to 4. The finial pressures in the reference cell ($P_{R,F}^{i}$) can also be controlled by regulating the CO_2 quality expanded into the sample cell from the reference cell with a needle valve between the two cells. $P_{R,I}^{i}$ and $P_{R,F}^{i}$ may be controlled in the region C (Fig. 2) for pressure points 5 to 15. The equilibrium pressures in the sample cell for the $(i-1)^{th}$ step ($P_{S,Eq}^{i-1}$) and i^{th} step ($P_{S,Eq}^{i}$)depend on the CO_2 quality expanded from the reference cell, the volumes of the two cells and the sorbed amount on coal. $P_{S,Eq}^{i-1}$ and $P_{S,Eq}^{i}$ are in the region A for pressure points 5 to 6. For pressure points 7 to 9, $P_{S,Eq}^{i-1}$ and $P_{S,Eq}^{i}$ are in the region B. $P_{S,Eq}^{i-1}$ and $P_{S,Eq}^{i}$ are in the region C for the pressure points 10 to 15.

From column (10) of Table 3, the $\left[\partial\rho/\partial P_{R,I}^{i}\right]_T$ values are from 0.164 to 1.063 mmol/(cm³·MPa) at $P_{R,I}^{i}$. The $\left[\partial\rho/\partial P_{R,F}^{i}\right]_T$ values for the reference cell are from 0.187 to 2.155 mmol/(cm³·MPa) at $P_{R,F}^{i}$ from column (11) of Table 3. From columns (12) and (13) of Table 3, the maximum $\left[\partial\rho/\partial P_{S,Eq}^{i}\right]_T$ and $\left[\partial\rho/\partial P_{S,Eq}^{i-1}\right]_T$ are from 0.229 to 5.672 mmol/(cm³·MPa). The density change of CO_2 with pressure at a constant temperature in the sample cell is obviously greater than that in the reference cell,

especially under medium pressure, which is caused by the operating conditions. The pressure in the reference cell may be controlled in the regions A and C of Fig. 2 by pressurization with the CO_2 booster-pump and the CO_2 quality expanded into the sample cell. However, equilibrium pressure in the sample cell is difficult to be controlled in the regions A and C, and region B is to be avoided, which is caused by CO_2 adsorption on coal and a greater $[\partial\rho/\partial P]_T$ value in the region.

The absolute value of $\left[\partial\rho/\partial T_{R,I}^{i}\right]_P$, $\left[\partial\rho/\partial T_{R,F}^{i}\right]_P$ and $\left[\partial\rho/\partial T_{S,Eq}^{i}\right]_P$ is from 0.012 to 0.231, 0.008 to 0.560 and 0.005 to 1.071 mmol/(cm³·K), respectively. Just like the effect of pressure accuracy, the influence of temperature accuracy in the sample cell on CO_2 adsorption error is greater than that in the reference cell.

As can be seen from Table 3, the value of the adsorption increment is negative as the equilibrium pressure is greater than 8.5 MPa. So, there is a maximum of total adsorption and the adsorption isotherm exhibits an obvious asymmetric parabolic shape.

Error analysis

Based on error propagation, the expected error limit of excess sorption increment at the ith expansion step due to the variable error is calculated with Eqs. (27) and (28) can be used to determine the error limit of excess total sorption at j^{th} step.

$$d\Delta n_i^{\text{ex}} = \Delta n_{P_{R,I}^i} + \Delta n_{P_{R,F}^i} + \Delta n_{P_{S,Eq}^i} + \Delta n_{P_{S,Eq}^{i-1}} + \Delta n_{T_{R,I}^i}$$
$$+ \Delta n_{T_{R,F}^i} + \Delta n_{T_{S,Eq}^i} + \Delta n_{T_{S,Eq}^{i-1}} + \Delta n_{V_R} + \Delta n_{V_0} + \Delta n_m \quad (27)$$

$$dn_j^{\text{ex}} = d\Delta n_1^{\text{ex}} + d\Delta n_2^{\text{ex}} + \cdots + d\Delta n_i^{\text{ex}} + \cdots + d\Delta n_j^{\text{ex}} \quad (28)$$

The excess CO₂ sorption increment, total sorption isotherms on the coal and their errors at 40°C are shown in Fig. 3 which displays the error limit (calculated with Eqns. (27) and (28)) with filled area plots, standard error (calculated with Eqns. (19) and (20)) with error bars, and sorption increment and total sorption with dotted line. The serial number in Fig. 3 indicates CO₂ expansion step as shown in Table 3.
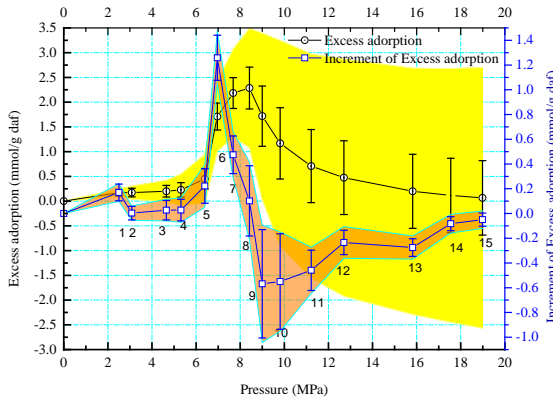
Fig. 3. The excess sorption increment and its isotherms (dotted line), error limit (filled area plot) and standard (error bar) errors of sorption increment and total sorption

The error limit of the adsorption increment calculated with Eq. (27) is greater than the standard error of the increment calculated with Eq. (19), especially at a pressure of 8-10 MPa. With pressure increase, the error limit of the increment increases to a maximum and then decreases. The maximum appears at an equilibrium pressure of 8.998 MPa, being consistent with the maximum $[\partial \rho / \partial P]_T$ of 5.672 mmol/(cm³·MPa) at 40°C. The increment error is very low at a pressure lower than 8 MPa (low pressure) and higher than 10 MPa (high pressure). The maximum error of sorption increment appears at a pressure with negative sorption increment. The negative increment at the ith step indicates the maximum sorption at the $(i\text{-}1)$th step. The reason why the negative increment or maximum sorption is at the maximum increment-error should be studied in the future.

The error limit of total adsorption calculated with Eqns. (27) and (28) has an extreme value, plotted with filled area in Fig. 3. The error limit is very great, accounting for 54% of the maximum adsorption. The negative adsorption will appear as negative error limit caused by pressure and temperature sensor accuracy, and the shape of the

adsorption isotherm will change as positive error-limit. The error of adsorption caused by the errors of the experimental parameters may result in a lower reproducibility and repeatability of supercritical CO₂ adsorption at high pressure.

Coal swelling effect on the measured adsorption of CO₂

Coal volumetric swelling caused by CO₂ adsorption is a well-known phenomenon [20, 21]. Firstly, the most reported maximum volumetric swelling of coal in CO₂ was within the range of about 1 to 5%, with highest swelling usually associated with lower-rank coals [22-27]. The corrected excess sorption was about 30% greater than the uncorrected value at 15 MPa.

In case of coal density of 1.27 g/cm³ (Table 1), the void volume decreases by 0.003, 0.04 and 0.08 cm³ per gram coal coal swelling of 0.4%, 5.0% and 10.0%, respectively. The error of the void volume in the sample cell is 0.033, 0.408, 0.815 cm³, corresponding to the coal swelling amount above, respectively. The errors caused by coal swelling are obviously greater than the errors in Table 2. The V_0 errors caused by the coal swelling of 0.4%, 5.0% and 10.0% are 2.5, 31.4 and 62.7 times the instrumental error, respectively.

The coal swelling volume of 0.4% has little influence on the accuracy of adsorption measurement. As the coal swelling volume is small in comparison with the void volume error, its effect on CO₂ adsorption is ignorable. So, a great volume of sample cell and a small coal mass (i.e. great specific void volume) may make us ignore coal swelling effect when coal swelling is not too large.

With the increase in the extent of coal swelling, its effect on adsorption measurement becomes greater. At a coal swelling volume of 10%, the influence of the swelling on the adsorption measurement is similar to that of the pressure at medium pressure, and the effect is even greater than that of the pressure at low and high pressure. Coal swelling of 5% or more will obviously increase the CO₂ adsorption, especially at low and high pressure.

Limitation of temperature control

Temperature increases or decreases in the two cells as a result of the Joule-Thompson effect during CO₂ expansion procedure [28]. The temperature of CO₂ in the reference cell will rise with CO₂ pressurization with the CO₂ booster-pump, CO₂ temperature will decrease in the cell when CO₂ is expanded into the sample cell from the cell. The temperature in the sample cell will rise when CO₂ is expanded into the cell from the reference cell.

Therefore, the temperature of the two cells is not always constant during the determination of the adsorption capacity. The CO_2 temperature in the two cells and the temperature of the coal sample in the sample cell depend on the operation process.

The effect of temperature sensor accuracy on the determination of CO_2 adsorption capacity is smaller than that of the pressure sensor, but the temperature of CO_2 gas, cell body, coal sample, valve and pipe connecting the two cells is difficult to be determined because the temperature is not always equal everywhere. has a The high Joule-Thomson coefficient of CO_2 [19] and the poor thermal conductivity of coal [29-31] can lead to a temperature gradient in the sample cell.

CONCLUSIONS

This study provides an experimental case about the limitation of measurements of supercritical CO_2 adsorption isotherms on coals with manometric equipment at high pressure. The contribution of pressure-sensor accuracy to the uncertainty of incremental adsorption is greater than that of temperature error at equilibrium pressure less than 10 MPa, and the contribution of temperature-sensor accuracy is greater than that of pressure at equilibrium pressure higher than 10MPa. The error of adsorption caused by pressure- and temperature-sensor accuracy may result in lower reproducibility and repeatability of supercritical CO_2 adsorption at high pressure, and negative adsorption and change of the shape of adsorption isotherm. Coal swelling will result in a volume change of the sample cell, and will lead to an obvious increase in CO_2 adsorption in case of large swelling extent of coal. Higher Joule-Thomson coefficient of CO_2 and poor thermal conductivity of coal and CO_2 can lead to a temperature gradient in the sample cell, which will result in a high error of supercritical CO_2 adsorption on coal.

REFERENCES

1. Y. Chen, X. Zhong, Q. Zhang, *Ind. Eng. Chem. Res.*, **51**, 9260 (2012).
2. Y. Chen, Q. Han, Y. Wang, Q. Zhang, X. Qiao, *J. Appl. Polym. Sci.*, **132**, 41723 (2015).
3. S. Sun, C. Liu, Y. Ye, *J. Chem. Thermodyn.*, **57**, 256 (2013).
4. S. Sun, C. Liu, Q. Meng, *J. Chem. Thermodyn.*, **84**, 1 (2015).
5. H. Yu, G. Zhou, W. Fan, J. Ye, *Int. J. Coal Geol.*, **71**, 345 (2007).
6. H. Yu, L. Zhou, W. Guo, J. Cheng, Q. Hu, *Int. J. Coal Geol.*, **73**, 115 (2008).
7. H. Yu, J. Yuan, W. Guo, J. Cheng, Q. Hu, *Int. J. Coal Geol.*, **73**, 156 (2008).
8. R. Jiang, H. Yu, L. Wang, *Bulg. Chem. Commun.*, **49**, 509 (2017).
9. Y. Gensterblum, P. van Hemert, P. Billemont, E. Battistutta, A. Busch, B.M. Krooss, G. De Weireld, K.-H.A.A. Wolf, *Int. J. Coal Geol.*, **84**, 115 (2010).
10. A.L. Goodman, A. Busch, R.M. Bustin, L. Chikatamarla, S. Day, G.J. Duffy, J.E. Fitzgerald, K. A.M. Gasem, Y. Gensterblum, C. Hartman, C. Jing, B.M. Krooss, S. Mohammed, T. Pratt, R.L. Robinson Jr., V. Romanov, R. Sakurovs, K. Schroeder, C.M. White, *Int. J. Coal Geol.*, **72**,153 (2007).
11. S.J.F. Mohammed, R.L. Robinson Jr., K.A.M. Gasem, *Energy Fuels*, **23**, 2810 (2009).
12. V.N. Romanov, A.L. Goodman, J.W. Larsen, *Energy Fuels*, **20**, 415 (2006).
13. R. Sakurovs, S. Day, S. Weir, I*nt. J. Coal Geol.*, **77**, 16 (2009).
14. P. van Hemert, E.S.J. Rudolph, J. Bruining, K.-H.A. A. Wolf, *SPE J.*, **15**, 146 (2010).
15. S. Hol, Y. Gensterblum, C. J. Spiers, *Fuel*, **105**, 192 (2013).
16. H. Yu, W. Guo, J. Cheng, Q. Hu, *Int. J. Coal Geol.*, **74**, 250 (2008).
17. R. Jiang, H. Yu, L. Wang, L. Chen, *Int. J. Smart Sens. Intell. Syst.*, **9**, 468 (2016).
18. D.F. Zhang, L.L. Cu, S.G. Li, P.C. Lian, J. Tao, *Int. J. Global Warming*, **5**, 197 (2013)
19. R. Span, W. Wagner, *J. Phys. Chem. Ref. Data*, **25**, 1509 (1996).
20. S. Day, R. Fry, R. Sakurovs, *Int. J. Coal Geol.*, **93**, 40 (2012).
21. E. Ozdemir, B. I. Morsi, K. Schroeder, *Langmuir*, **19**, 9764 (2003).
22. N. Siemons, A. Busch, *Int. J. Coal Geol.*, **69**, 229 (2007).
23. G. Ceglarska-Stefańska, A. Czapliński, *Fuel*, **72**, 413 (1993).
24. S. Day, R. Fry, R. Sakurovs, S. Weir, *Energy Fuels*, **24**, 2777 (2010).
25. P. Chareonsuppanimit, S. A. Mohammad, R. L. Robinson Jr., K. A. M. Gasem, *Int. J. Coal Geol.*, **12**1, 98 (2014).
26. P. J. Reucroft, H. Patel, *Fuel*, **65**, 816 (1986).
27. P. J. Reucroft, A. R. Sethuraman, *Energy Fuels*, **1**, 72 (1987).
28. C.M. Oldenburg, *Energy Convers. Manag.*, **48**, 1808 (2007).
29. B. Tian, Y. Qiao, Y. Tian, Q. Liu, *J. Appl. Pyrol.*, **121**,376 (2016).
30. Y. Zhang, J. Zhu, X. Wang, X. Zhang, S. Zhou, P. Liang, *Fuel Process. Technol.*, **154**, 227 (2016).
31. X. Qu, P. Liang, Z. Wang, R. Zhang, D. Sun, *Chem. Eng. Technol.*, **34**, 61 (2011)